SCIENCE CHINA
Earth Sciences

• RESEARCH PAPER •

July 2014 Vol.57 No.7: 1480–1493
doi: 10.1007/s11430-013-4801-4

Impacts of boundary layer parameterization schemes and air-sea coupling on WRF simulation of the East Asian summer monsoon

WANG ZiQian[1,2,3], DUAN AnMin[1*] & WU GuoXiong[1]

[1] *State Key Laboratory of Numerical Modeling for Atmospheric Sciences and Geophysical Fluid Dynamics, Institute of Atmospheric Physics, Chinese Academy of Sciences, Beijing 100029, China;*
[2] *Key Laboratory for Land Surface Process and Climate Change in Cold and Arid Regions, Chinese Academy of Sciences, Lanzhou 730000, China;*
[3] *University of Chinese Academy of Sciences, Beijing 100049, China*

Received March 8, 2013; accepted September 6, 2013; published online April 8, 2014

The planetary boundary layer (PBL) scheme in the regional climate model (RCM) has a significant impact on the interactions and exchanges of moisture, momentum, and energy between land, ocean, and atmosphere; however, its uncertainty will cause large systematic biases of RCM. Based on the four different PBL schemes (YSU, ACM2, Boulac, and MYJ) in Weather Research and Forecasting (WRF) model, the impacts of these schemes on the simulation of circulation and precipitation during the East Asian summer monsoon (EASM) are investigated. The simulated results of the two local turbulent kinetic energy (TKE) schemes, Boulac and MYJ, are more consistent with the observations than those in the two nonlocal closure schemes, YSU and ACM2. The former simulate more reasonable low-level southwesterly flow over East China and west pacific subtropical high (WPSH) than the latter. As to the modeling of summer monsoon precipitation, both the spatial distributions and temporal evolutions from Boulac and MYJ are also better than those in YSU and ACM2 schemes. In addition, through the comparison between YSU and Boulac experiments, the differences from the results of EASM simulation are more obvious over the oceanic area. In the experiments with the nonlocal schemes YSU and ACM2, the boundary layer mixing processes are much stronger, which lead to produce more sea surface latent heat flux and enhanced convection, and finally induce the overestimated precipitation and corresponding deviation of monsoon circulation. With the further study, it is found that the absence of air-sea interaction in WRF may amplify the biases caused by PBL scheme over the ocean. Consequently, there is a reduced latent heat flux over the sea surface and even more reasonable EASM simulation, if an ocean model coupled into WRF.

WRF model, boundary layer parameterization scheme, East Asian summer monsoon, air-sea coupling

Citation: Wang Z Q, Duan A M, Wu G X. 2014. Impacts of boundary layer parameterization schemes and air-sea coupling on WRF simulation of the East Asian summer monsoon. Science China: Earth Sciences, 57: 1480−1493, doi: 10.1007/s11430-013-4801-4

As one of the important components of the Asian summer monsoon, the variation of East Asian summer monsoon (EASM) influences the weather and climate change over China and its adjacent areas (Li et al., 2003; Tao et al., 1997). In recent years, the climatic disaster events occurred frequently over China due mainly to the anomalous EASM, which caused huge economic losses and casualties. The regional climate model (RCM) has higher resolution that can represent the more accurate topography and reasonable land surface process, and it is a useful tool in the study of weather and climate change over East Asia. However, there are still large uncertainties in the EASM simulation using the RCM, particularly the simulation of monsoon precipitation (Fu et al., 2005; Feng et al., 2007).

The uncertainties from the model physical parameterization schemes are one of the primary causes to the systemic error in RCM, such as the schemes of cumulus convection, land surface process, and planetary boundary layer (PBL).

*Corresponding author (email: amduan@lasg.iap.ac.cn)

Most previous studies focused on the evaluation of the impacts from cumulus convection parameterization schemes on the simulated results (e.g., Wang et al., 1997; Liu et al., 2001a; 2001b; Emori et al., 2001; Gochis et al., 2002; Lee et al., 2005; Mukhopadhyay et al., 2010; Yu et al., 2012). Except for the cumulus convection, the imperfect PBL scheme can also cause large systematic biases; this is because the PBL scheme in RCM has a significant impact on the interactions and exchanges of moisture, momentum, and energy between land, ocean, and atmosphere.

A few recent studies have examined the sensitivity of the weather and climate simulation to the PBL schemes. Based on the fifth-generation Mesoscale Model (MM5), Zhang et al. (2004) conducted a comparative numerical modeling study of summertime weak-gradient flows with five widely used PBL parameterization schemes over the central United States; results showed that the nonlocal Blackadar scheme has the best reproduction of the diurnal cycles of surface wind. Hu et al. (2010) tested three PBL schemes (MYJ, YSU, and ACM2) of Weather Research and Forecasting (WRF) model in the summer of 2005 over south-central United States. They concluded that MYJ scheme has weaker entrainment processes at the top of PBL due to the weaker vertical mixing, thus resulting in lower temperature and higher moisture near the surface than other two PBL schemes. Similarly using WRF model, Flaounas et al. (2011) indicated that MYJ PBL scheme simulates more reasonable moisture and temperature after comparing it with the YSU scheme in the simulation of the West Africa summer monsoon in 2006. But in the simulated study of 1998 EASM with SUNRCM regional model, Cha et al. (2008) found the improved YSU PBL scheme has a better performance than the old version MRF, where the main reason is the weakening vertical mixing in YSU scheme. In addition, Liu (2006) compared the performances of YSU and MYJ PBL schemes in the simulation of the summer precipitation in 1998 over East China using the climatic version of WRF model (CWRF (Liang et al., 2012)). The comparison shows that there is little difference in the rainband distribution and the daily variation of the area-averaged rainfall between the two PBL schemes, but significant difference in the distribution of heavy rainfall over the low vortex and shear line. Because of the unpublished CWRF, the users cannot obtain the CWRF code easily. On the other side, with the continuous development and improvement of WRF model, more and more researchers used the WRF model as an RCM to study the EASM in recent years (e.g., Wang et al., 2008; Kim et al., 2010; Kim et al., 2011; Yang et al., 2011; Liu, 2012; Yu et al., 2012). Nevertheless, the impact of different PBL schemes in WRF model on the simulation of EASM has received no attention.

This study will investigate the impacts of four widely used PBL parameterization schemes in WRF model on EASM simulation in the period of 2000–2009, and discuss the possible reason for the simulated biases. The four PBL schemes include two nonlocal closure schemes YSU (Yonsei University scheme) (Hong et al., 2006) and ACM2 (Asymmetric Convective Model version 2) (Pleim, 2007a; 2007b), and two local turbulent kinetic energy (TKE) schemes BouLac (Bougeault-Lacarrere) (Bougeault et al., 1989) and MYJ (Mellor-Yamada-Janjic) (Janjic, 1990; 2002). The results can provide reference on the choice of PBL schemes when the WRF model is used to do any work about EASM, and also have value to the improvement of WRF model in the future.

1 The model and experimental design

The model used in this study is the non-hydrostatic Advanced Research WRF model (version 3.4), which has been widely employed to the prediction and research of the weather and climate. At present, various PBL schemes are provided in WRF, which can be roughly divided into local and nonlocal schemes. Here, we choose the two widely used nonlocal schemes — YSU and ACM2, and two local schemes—BouLac and MYJ, and explore their impacts on the simulation of EASM.

YSU characterized as a classic nonlocal closure PBL scheme is improved from the Medium-Range Forecast (MRF) scheme (Hong et al., 1996), in which the critical revision is that the treatments of the entrainment process become explicit at the top of PBL. Based on the large eddy simulation data, the entrainment is expressed as a variable proportionally with the surface buoyancy flux. The PBL height in YSU is defined at the height where the Richardson number is zero. Perhaps, YSU is the most popularly used scheme in the previous studies. ACM2 is a combination of ACM1 and an eddy diffusion model, which treats nonlocal fluxes using a transilient matrix (Holtslag et al., 1993). ACM2 is intended to be more applicable to trace and simulate the humidity, winds, temperature and chemical mixing ratios in the boundary layer. As to the local scheme, MYJ is constructed on the basis of the 1.5-order (level 2.5) turbulence closure model of Mellor and Yamada (Mellor et al., 1982). The MYJ scheme determines the vertical mixing process in PBL and free atmosphere through the local TKE, and requires one additional prognostic equation of the TKE. This TKE closure scheme applies the local mixing with local diffusivity from the lowest to the highest level for both convective and stable boundary layer. Similar to the MYJ, BouLac is also a local TKE scheme, and they just differ in how to define the empirical constants of proportional coefficient and mixing length. Meanwhile, the local schemes BouLac and MYJ estimate the turbulent fluxes at each grid point only from the mean values of atmospheric variables and their gradients at that grid point. However, the surrounding grid points are also considered in the nonlocal YSU and ACM2 schemes.

Four ensemble experiments were performed with the

above different PBL schemes respectively, and the other physical parameterization schemes in WRF model include: the WRF single-moment six-class (WSM-6) cloud microphysics scheme, the Grell–Devenyi (GD) convective scheme, the NOAH land-surface model, a Goddard shortwave scheme, and the Rapid Radiative Transfer Model (RRTM) for longwave radiation. Each of the ensemble experiments has ten summers (2000–2009) with the initial modeling conditions at 0000UTC April 22, and ends at 1800UTC August 31. The days before May 1 were considered a "spin-up" period (Giorgi et al., 1999), and the output in last four months were analyzed. The simulation domain covers most parts of Asia and adjacent oceans with 181 grid points along the east-west direction and 131 along the north–south direction (the buffer zone has 10 grid points). A Lambert projection is adopted and the domain is centered at 30°N, 102.5°E. The model has a 45 km horizontal resolution and 35 vertical layers with a terrain-following sigma coordinate and a prescribed model top at 10 hPa. Figure 1 shows the model domain and topography map.

The initial state of the atmosphere and the lateral boundary conditions (updated every 6 hours) in WRF are derived from National Centers for Environmental Prediction final analysis data (NCEP-FNL, http://rda.ucar.edu/datasets/ds083.2/) with a 1°×1° horizontal resolution. The daily Optimum Interpolated Sea Surface Temperature (OISST, ftp://eclipse.ncdc.noaa.gov/pub/OI-daily-v2) on a 0.25°×0.25° grid was also used to drive the WRF. We applied Tropical Rainfall Measuring Mission (TRMM) 3B42 rainfall data (Huffman et al. 2007), with a 3-h temporal resolution and 0.25°×0.25° horizontal resolution; these data can reflect the monsoon precipitation reasonably over the East Asian (Mao et al., 2012). Additionally, the daily precipitation records from 2518 stations over China during the period of 2000–2009 provided by the China Meteorological Administration (CMA) were used to compare with the simulated results. The WRF output simulations and all the observational data were spatially re-gridded onto 0.5°×0.5° grid points through the bilinear interpolation method.

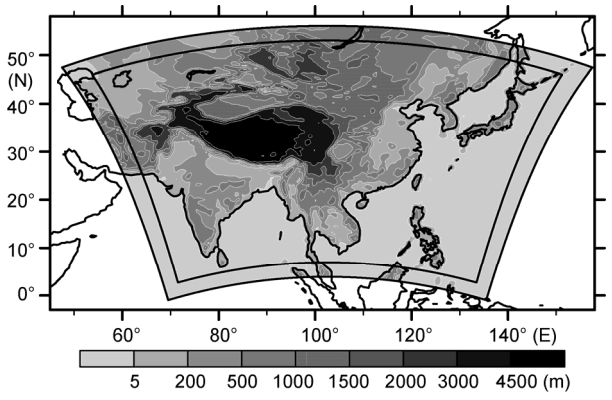

Figure 1 The WRF model domain and topography map (m). The area lapped by the solid lines at the boundary is the buffer zone.

2 Results

In this part, the simulated results of monsoon circulation and precipitation were compared with the observations, in order to investigate the WRF's performance in simulating EASM and the impacts of different PBL schemes on the modeling results.

2.1 Large-scale circulation

Figure 2 shows the spatial distributions of JJA (June-July-August, 2000–2009) mean wind at 850 hPa from NCEP-FNL and the four different PBL schemes (YSU, ACM2, BouLac and MYJ). All the four schemes can reproduce well the cyclonic circulations over south of the Tibetan Plateau (TP), which are induced by the TP's thermal effect (Wu et al., 2012). They also capture the fields of the low-level southwesterly jet over the Bay of Bengal (BOB), the South China Sea (SCS), and the northwest Pacific, although the wind speeds are somewhat stronger than that in the NCEP-FNL data; while the biases in YSU and ACM2 schemes are more obvious. There is always low-level southwesterly over East China in the summertime, and the western wind at 850 hPa changes to be southerly in east of the TP because of the topography. The schemes of BouLac and MYJ well capture the low-level monsoon southwesterly over East China and the southerly in east of the TP, but these characters cannot be reasonably expressed in the YSU and ACM2, particularly in ACM2 where there is no southwestern monsoon circulation over East China. In addition, the western Pacific subtropical high (WPSH) is the main circulation system over the northwest Pacific in summer (Figure 2(a)), which effects the distribution of monsoon rainband in China (Zhu et al., 2000). The simulated monsoon southwesterly over the northwest Pacific is stronger and WPSH is located more eastwardly in YSU and ACM2, while the WPSH circulations in BouLac and MYJ agree with NCEP-FNL better. The statistical results of zonal wind at 850 hPa (U850) over the EASM region (Table 1) show that, both the spatial correlation coefficient and the root mean square error (RMSE) in Boulac and MYJ are better than those in YSU and ACM2.

Figure 3 illustrates the distributions of JJA mean 500 hPa wind. It is shown that the main circulations in the observation (NCEP-FNL) include the shallow trough over northeastern China, WPSH, low vortex over the TP, and cyclonic system in the north of BOB. These systems can be generally simulated by the four PBL schemes; however, the WPSH anticyclonic is weaker and the cyclone in BOB is much stronger in YSU and ACM2 schemes after being compared with the observation. Similarly with 850 hPa, the modeling tropical southwesterly at 500 hPa is more vigoroso in YSU and ACM2 over Indo-China Peninsula and SCS, which is inconsistent with the observation. On the contrary, the results of BouLac and MYJ match the observation more

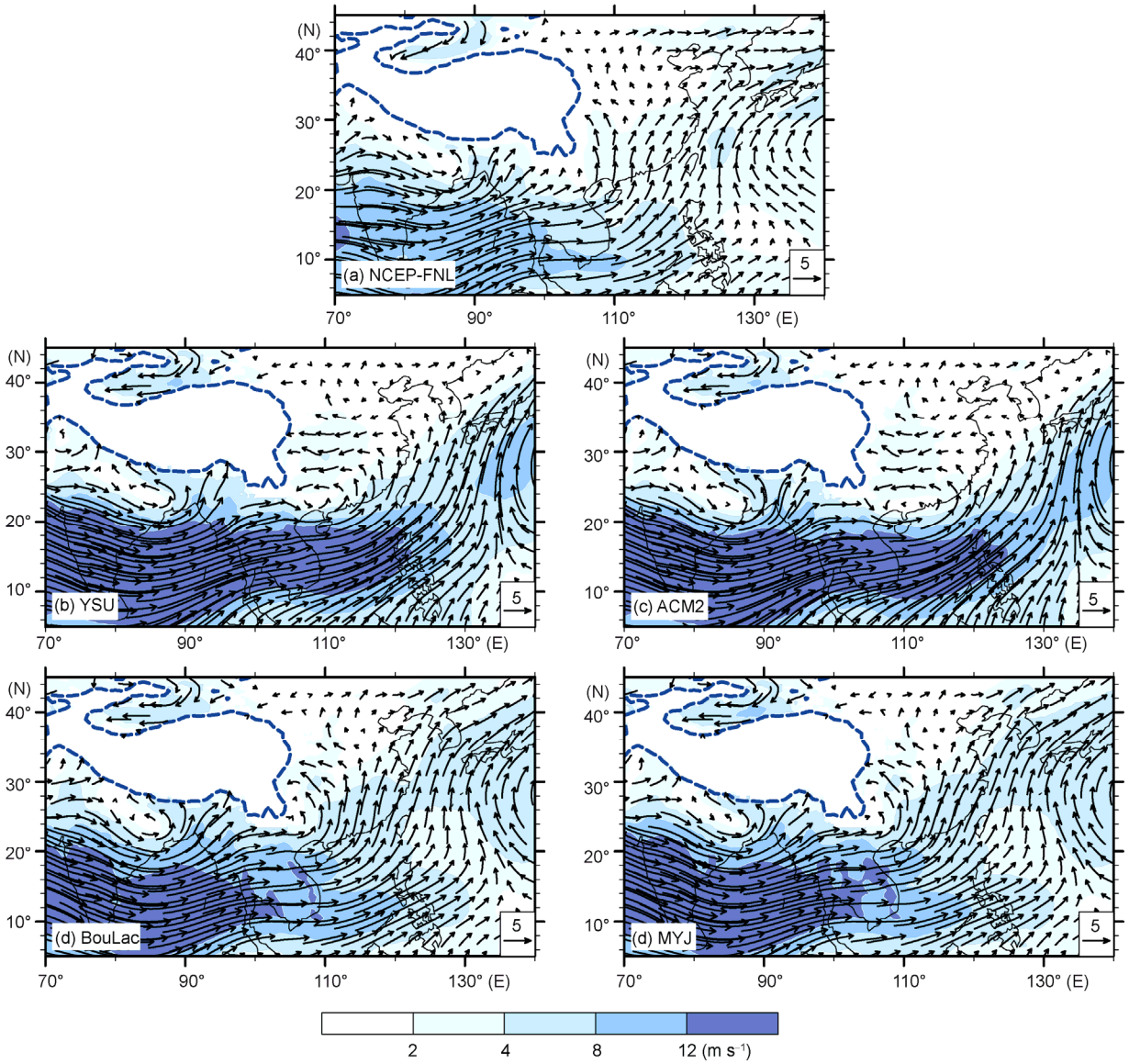

Figure 2 JJA mean wind fields (m s^{-1}) at 850 hPa during 2000–2009 from (a) NCEP-FNL; (b) YSU; (c) ACM2; (d) BouLac; (e) MYJ. The shaded indicates the wind speed, and the dash line marks the terrain height of 2000 m (the same in the following figures).

Table 1 JJA mean spatial correlation coefficient and RMSE over the East Asian monsoon area (10°–40°N, 105°–135°E)[a)]

		YUS	ACM2	BouLac	MYJ
U850	R	0.614	0.622	0.823	0.821
	RMSE	4.810	4.851	2.236	2.310
q850	R	0.904	0.898	0.944	0.941
	RMSE	0.827	1.196	0.503	0.528
PR	R	0.594	0.477	0.631	0.621
	RMSE	5.320	6.784	2.601	2.807

a) U850 is the zonal wind at 850 hPa (m s^{-1}), q850 is the water vapor mixing ratio at 850 hPa (g kg^{-1}), and PR is the precipitation (mm day^{-1}).

closely (Figure 3(d) and (e)). Furthermore, from the circulation at 200 hPa, it is indicated that the impacts of different PBL schemes on the upper-level atmosphere are unapparent (figure not shown).

2.2 Precipitation

Figure 4 demonstrates the distribution of the observed and simulated JJA mean precipitation for the period of 2000–

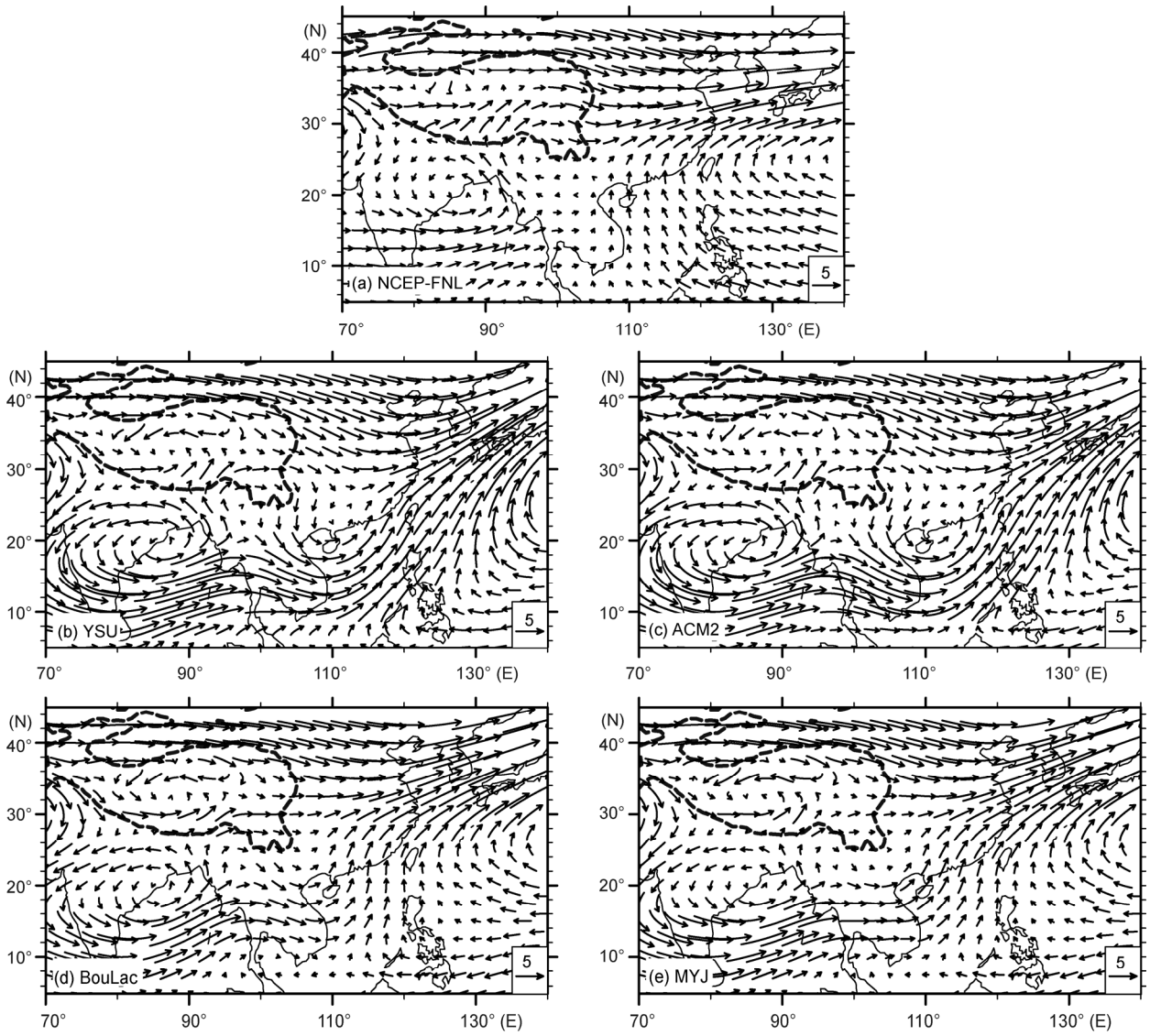

Figure 3 JJA mean wind fields (m s^{-1}) at 500 hPa during 2000–2009 from (a) NCEP-FNL; (b) YSU; (c) ACM2; (d) BouLac; (e) MYJ.

2009. WRF well reproduces the geographical pattern of monsoon rainfall, but the rainfall amount is overestimated. Particularly, the two nonlocal schemes YSU and ACM2 produce much more precipitation over the oceanic regions (BOB, SCS and the Western Pacific (WP)); these deviations correspond with the stronger low-level southwesterly (Figure 2(b) and (c)), and the more eastern location of WPSH that has been discussed in the former part. Nevertheless, dry biases exist over the Yangtze and Huaihe River basins in both YSU and ACM2 schemes, which are induced by the unsuccessful modeling of the low-level southwesterly over East China. Because the moisture conditions over the northern of Yangtze River are supplied mainly through the southwesterly. Based on the comparison, the oceanic precipitations in both BouLac and MYJ schemes are greatly reduced, and the rainfall over the Yangtze and Huaihe River basins is closer to the observation due to the better simulation of the low-level southwesterly over East China. The statistical results (Table 1) also indicate that the local BouLac and MYJ schemes perform better than the other two schemes in the simulation of spatial distributions of moisture at 850 hPa (q850) and precipitation (PR). Whereas the differences in the monsoon rainfall are most obvious, the BouLac scheme shows an optimal performance in which the spatial correlation coefficient is 0.631 and RMSE is just 2.601 mm day^{-1}.

A dominant feature of the summer precipitation over East China is that the rainband shifts from the south to north following the onset and northward boost of EASM. The latitude-time cross-sections of daily precipitation along 105°–122°E from May to August for 2000–2009 are illustrated in Figure 5. Figure 5(a) shows that the monsoon rainfall starts in South China in May with the development of SCS summer monsoon, and then gradually enhances and

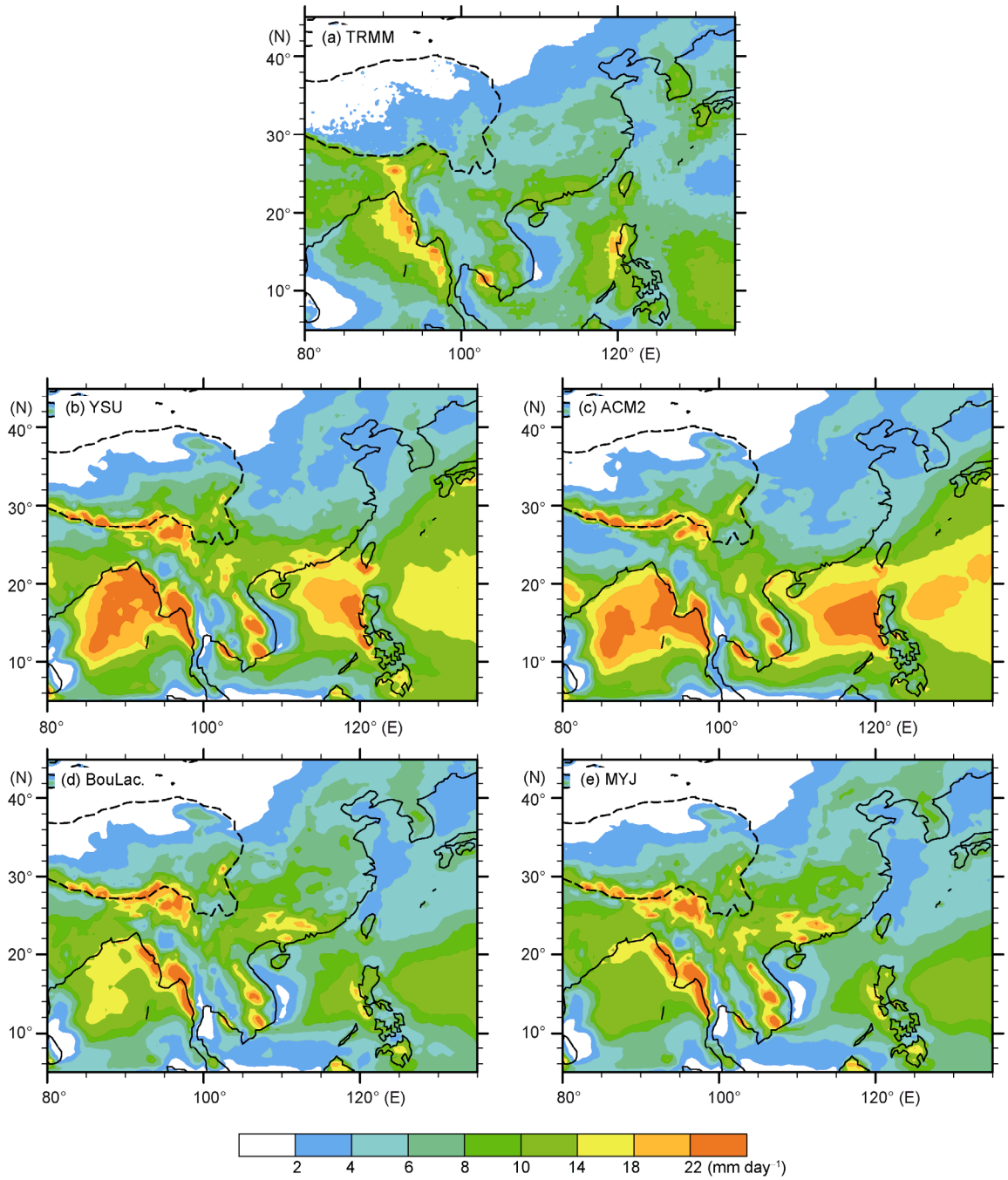

Figure 4 JJA mean precipitation (mm day^{-1}) during 2000–2009 from (a) TRMM; (b) YSU; (c) ACM2; (d) BouLac; (e) MYJ.

moves northwardly. It reaches the Yangtze River in June and North China in July and August, and then it retreats to the south of China in the late August. All the four PBL schemes underestimate the precipitation over South China in early May, but well simulate the northward shift in June. In YSU and ACM2 schemes, the maintaining of rain belts over the north of 30°N in July is not reproduced; moreover, the time of southward retreat is much earlier and dry biases occur over the Yangtze and Huaihe River basins. The results in BouLac and MYJ are better and more consistent with TRMM, particularly in BouLac scheme. Additionally, the simulated precipitations from both YSU and ACM2 are obviously stronger over the southern coastal area and SCS (around 20°N) during the whole modeling period. To further investigate the WRF performance of the temporal evolution of daily precipitation averaged from the different region over East China, Figure 6 describes the area-averaged daily rainfall over the north and south of Yangtze River respectively. The variation trends of EASM precipitation basically can be captured by all the four PBL schemes, and

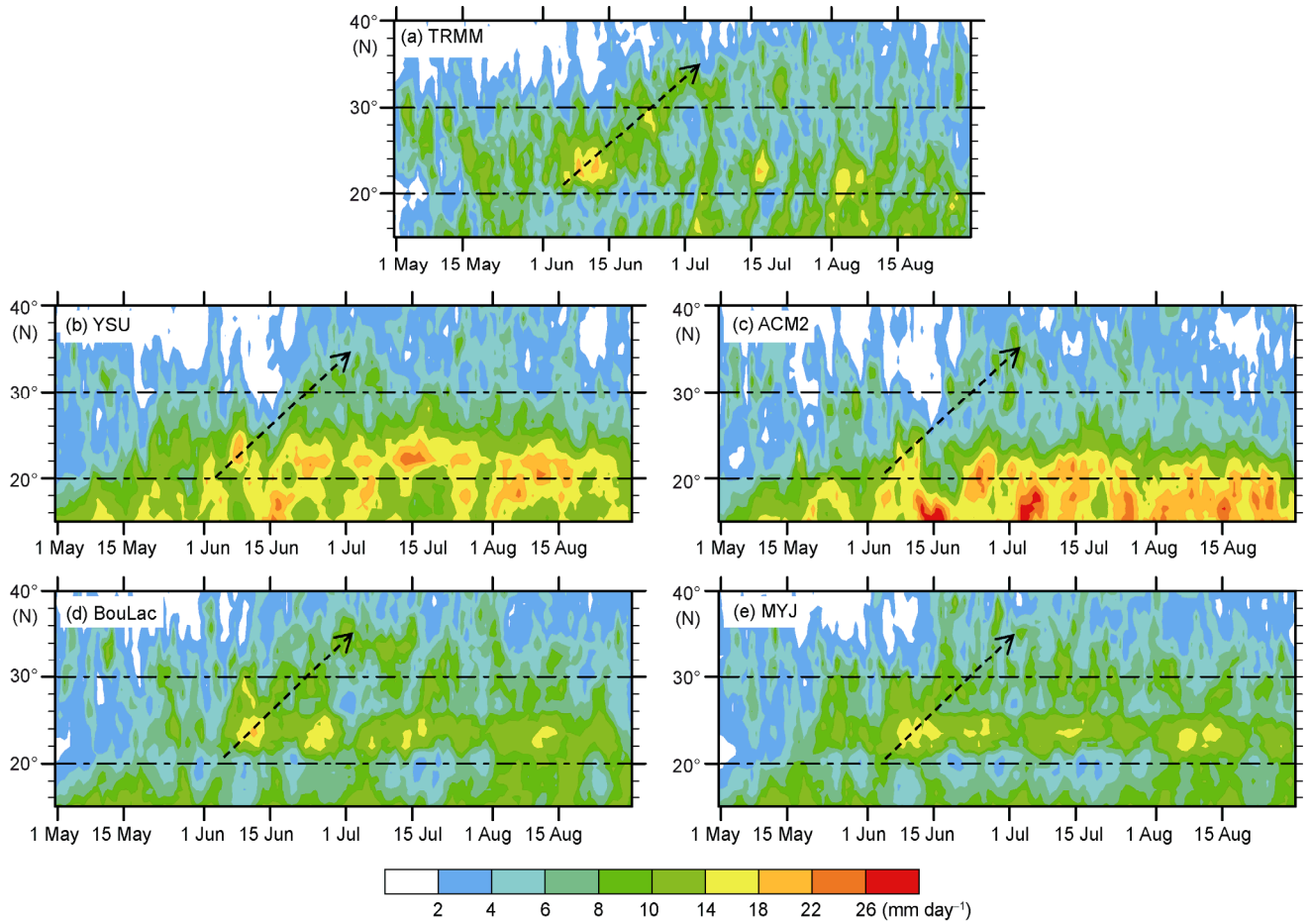

Figure 5 The latitude-time cross-sections of daily precipitation (mm day^{-1}) over East China (105°–122°E) for May to August. (a) TRMM; (b) YSU; (c) ACM2; (d) BouLac; (e) MYJ.

the results of the north Yangtze River area are better than south, which can be verified by the correlation coefficient. Figure 6 also shows that the dry biases of precipitation exist in the region north of 30°N, while large wet biases exist in the south area from YSU and ACM2 schemes. This is consistent with the results in Figure 4 and 5. By and large, the modeling temporal variations of the daily rainfall in BouLac and MYJ have better correlations with the observation than those in YSU and ACM2; the former can better reflect the intraseasonal variation characters of the summer precipitation over different area.

3 Reasons for the impacts of PBL schemes on the EASM simulation

In the last part, the WRF simulations of circulation and precipitation have been compared with the observation. Overall, the simulated results in the nonlocal schemes YSU and ACM2 are close to each other, whereas those in the other two local TKE schemes are also similar to each other. But the WRF performances of EASM simulation in BouLac and MYJ are much better than those in YSU and ACM2. Here, we choose the two schemes—YSU and BouLac, and try to compare their differences to investigate the possible reasons for the impacts of PBL parameterization on the EASM simulation.

Figure 7 shows the differences between YSU and BouLac schemes, including JJA mean wind and geopotential height at 850 hPa, precipitation, total moisture flux and its divergence from the surface to 300 hPa, and vertical velocity at 500 hPa. The simulated southwesterly jet over the area of BOB-SCS-WP is much stronger in YSU than BouLac, while the low-level southwesterly over East China and Korean Peninsula is weaker; thus an obvious cyclonic circulation is produced between YSU and BouLac over the EASM region. As to the precipitation (Figure 7(b)), the positive centers are located in the northeastern BOB, SCS and WP, but negative in the most of Chinese mainland. The difference of precipitation corresponds with the deviation of low-level monsoon circulation, which is also indicated from the moisture flux field (Figure 7(c)). The southwestern monsoon is stronger in YSU scheme, which leads to more supply of moisture with a remarkable moisture convergence, after that the upward motion is enhanced that means the

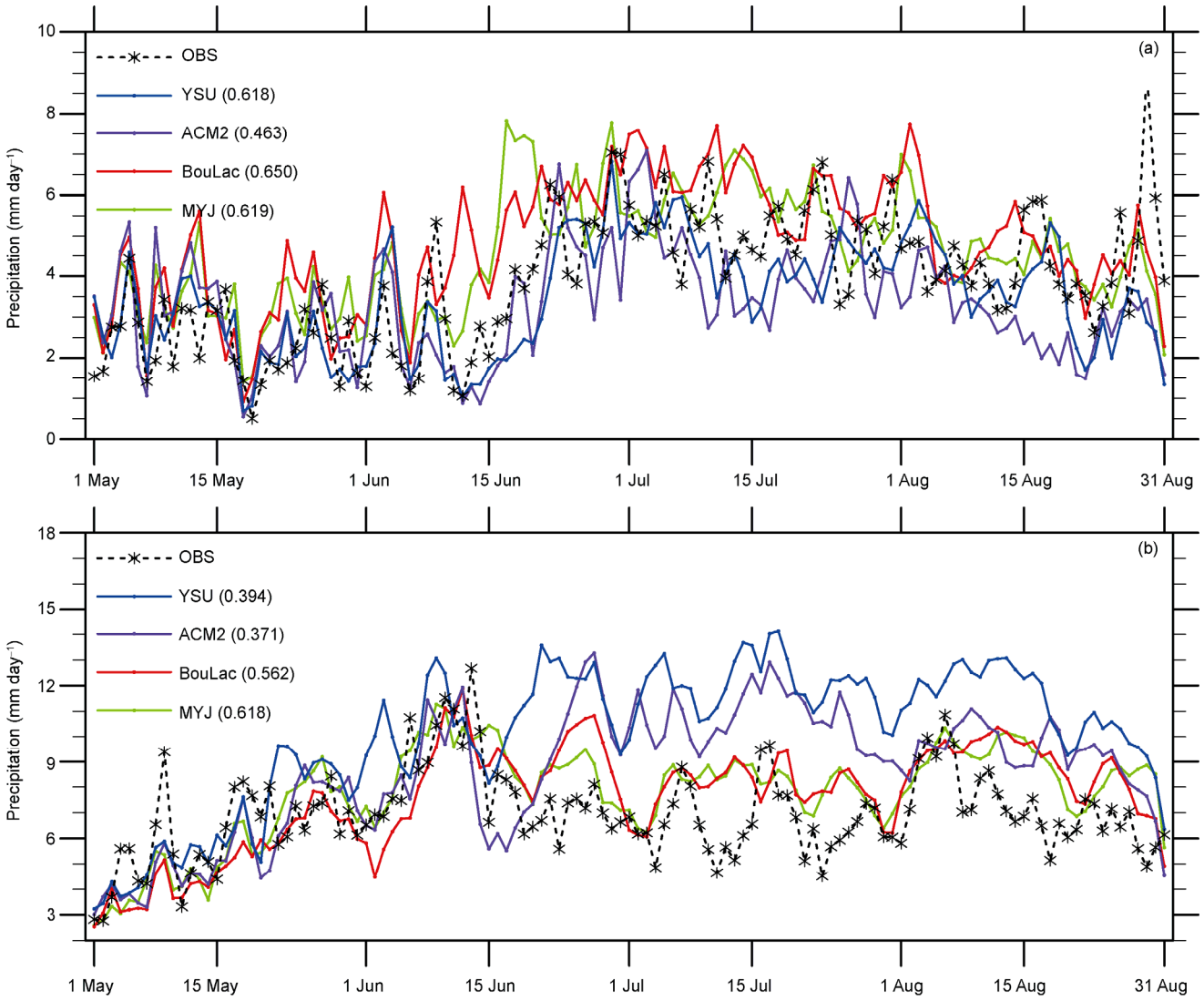

Figure 6 The time series of area-averaged daily precipitation for May to August over (a) north of the Yangtze River (30°–40°N, 105°–122°E), and (b) south of the Yangtze River (18°–30°N, 105°–122°E); where the OBS is calculated from the station precipitation data provided by CMA (the oceanic gird is filled by TRMM data), the numbers in the brackets are the correlation coefficient between the simulations and observation.

growth of convective activity. At the same time, the modeling of low-level southwesterly fails over East China in YSU, which results in less moisture transport from south, and then less rainfall. It is worth note that the differences in Figure 7 are more obvious over the ocean than over the land.

PBL mainly has the forcing effect in the vertical transport of moisture, heat or other variables and the release of condensation latent heat, and the PBL height is an important parameter in the related research (Nielsen et al., 2008). The difference of JJA mean PBL height between the two schemes is calculated in Figure 8(a), and the result in YSU is almost higher than that in BouLac over the whole domain. The positive PBL height implies the moisture and heat can be diffused in a larger space, which indirectly indicates that the PBL vertical mixing of YSU is stronger in East Asian region. Moreover, the YSU scheme has displayed a stronger vertical mixing effect in some previous studies in North America (Hu et al., 2010; Margaret et al., 2011). Figure 8 also shows the vertical profiles of the JJA mean potential temperature (a) and water vapor mixing ratio (b) in the reference area, and the values are averaged over land and over ocean respectively. The altitudinal variations of the potential temperature and moisture over both the ocean and land are smaller from the YSU scheme. This means that the YSU indeed simulates stronger PBL mixing as compared to the BouLac scheme. As a result, more moisture from the boundary layer in YSU can be transported to the free atmosphere; the simulated moisture by YSU is larger than that in BouLac at the higher levels (Figure 8(c)). Especially over the oceanic area, where more abundant moisture is supplied, the results at all levels in YSU exceed those in BouLac.

Due to the more abundant moisture supply in YSU scheme and together with the effect of strong wind stress,

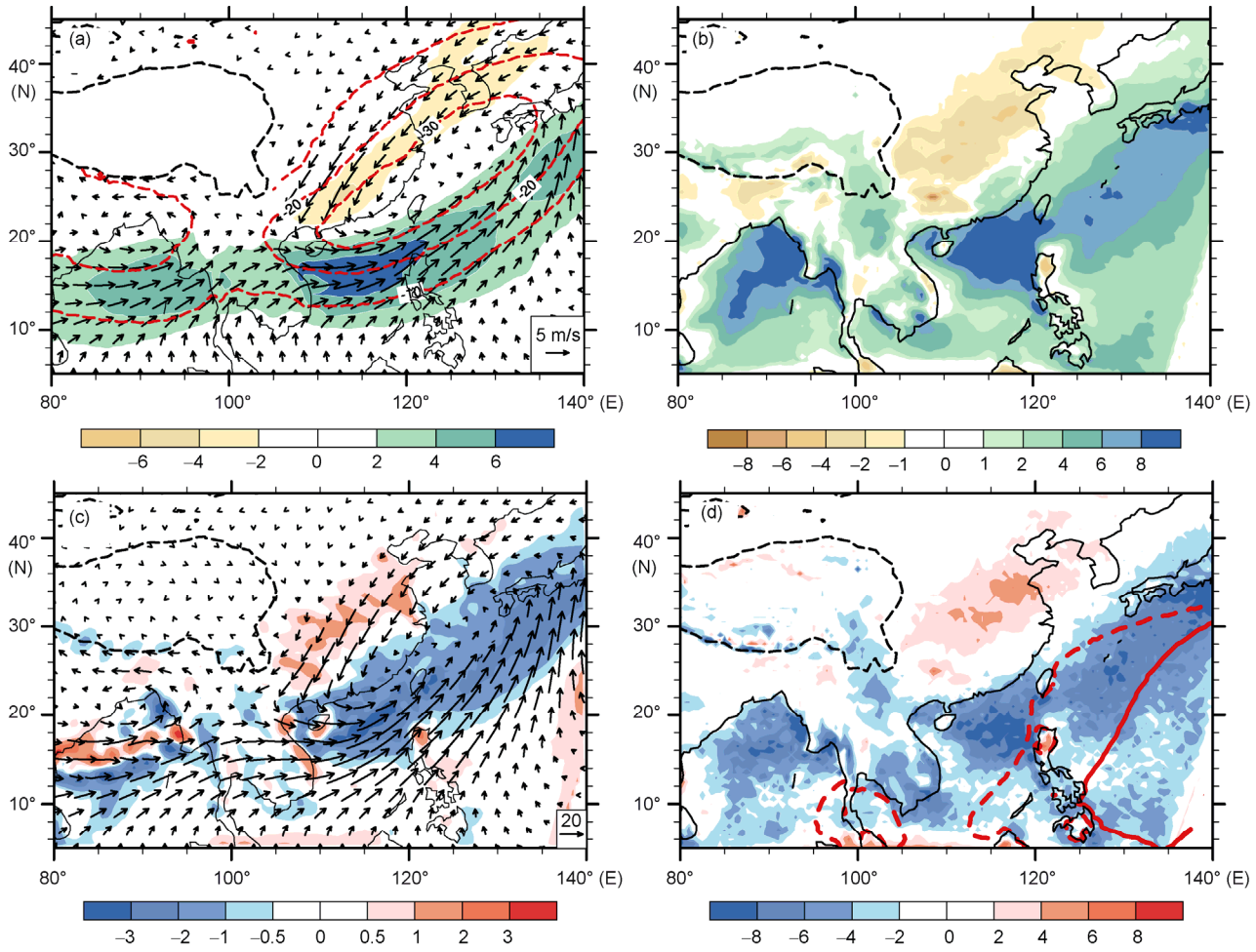

Figure 7 The differences of simulated results between YSU and BouLac in JJA. (a) wind (m s^{-1}) and geopotential height (contour, m) at 850 hPa; (b) precipitation (mm day^{-1}); (c) total moisture flux (kg m^{-1} s^{-1}) and its divergence (shaded, 10^{-5} kg m^{-2} s^{-1}) from the surface to 300 hPa; (d) vertical velocity (10^{-2} Pa s^{-1}) at 500 hPa, the red solid line is the 5880 gpm geopotential height in YSU scheme, and the dashed is in BouLac scheme.

more upward latent heat is induced from the surface (Figure 9(a)). Thus the wet enthalpy in lower troposphere is increased (Figure 9(b)), which enhances the atmospheric instability. Meanwhile, the more latent heat leads to stronger low-level diabatic heating, and then transforms into the increase of convective available potential energy (CAPE). As shown in Figure 9(c), the values of the transformed term $-(R/p)\omega T$ (where R is the gas constant of air, P is 700 hPa, ω is the vertical velocity, and T is the temperature) from CAPE to kinetic energy (Qort, 1964; Wu et al., 2012; Guan, 2010) are obviously positive over the oceanic area. It is indicated that more CAPE transforms into kinetic energy in the YSU scheme and results in stronger convective activity. This can be proved also by the vertical profiles of temperature and moist adiabat in Figure 9(d), and the simulated CAPE in YSU (2129 J) is larger than that in BouLac (1847 J). Therefore, the enhanced convection over the SCS and WP leads to overestimating the convective precipitation in YSU scheme. The atmospheric circulation also modulates adaptively at the same time and along with the decrease of the geopotential height (Figure 7(a)) that inhibits the westward expansion of the simulated WPSH (the 5880 gpm line in Figure 7(d)). In the lower troposphere, the more eastern location of the modeling WPSH induces weaker southwesterly in East China, but much stronger southwestern monsoon over the Northwest Pacific (Figure 2(b) and (c)). Moreover, the enhanced low-level wind can further strengthen the PBL vertical mixing over the oceanic area, and in turn the WRF accumulated error gets larger and larger.

According to the above analysis, the intensity of PBL mixing in the YSU scheme is stronger, which induces the more upward latent heat flux, more active convection and precipitation over the oceanic area, and adaptive modulation of the circulation at middle-low troposphere. Additionally, the results in ACM2 are similar to those in YSU, namely PBL vertical mixing is also stronger. On the contrary, mixing processes in MYJ and BouLac schemes are weaker, and

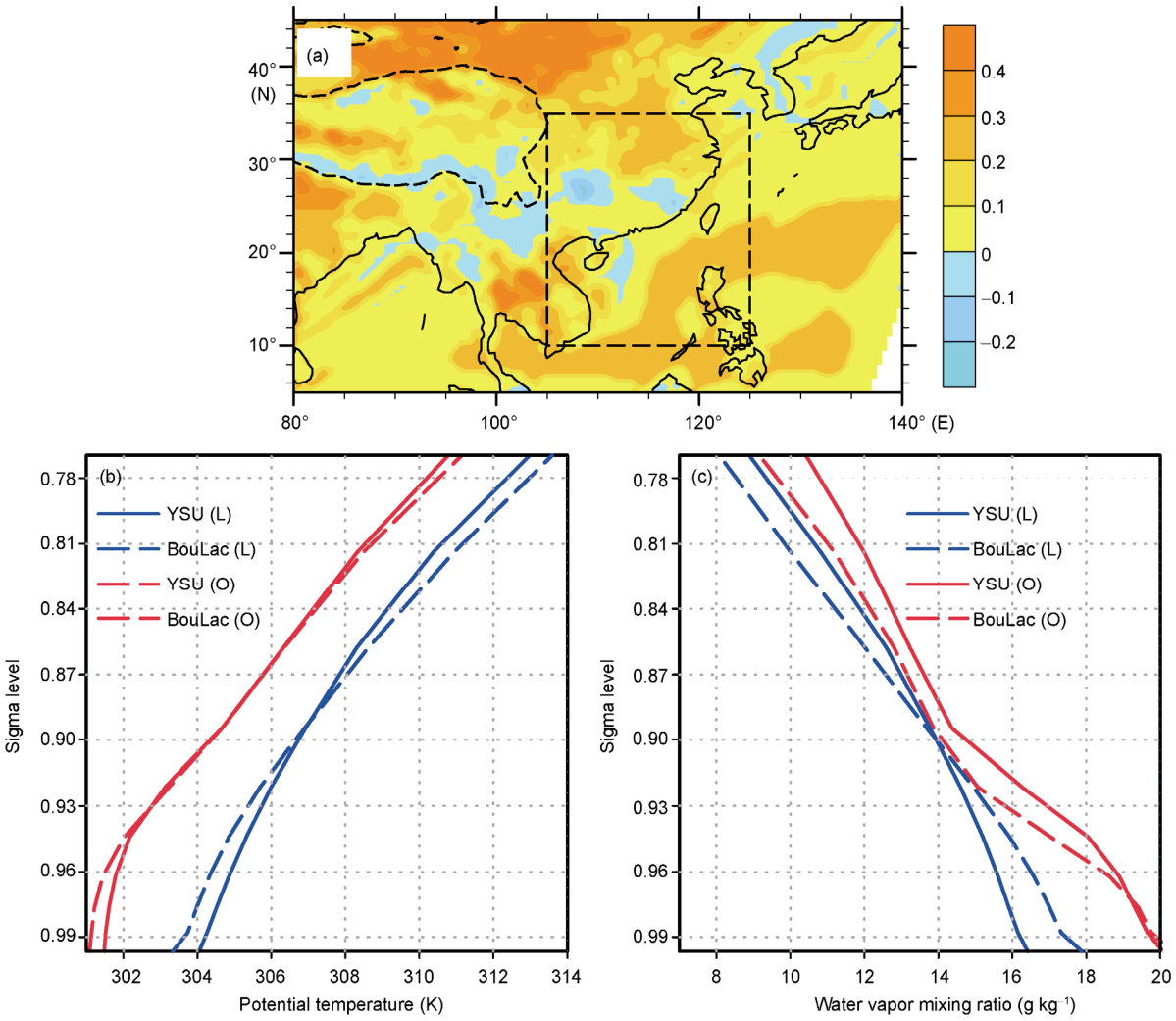

Figure 8 (a) The difference of PBL height (km) between YSU and BouLac in JJA; the vertical profiles of area averaged (the reference area marked in (a)) (b) potential temperature (K) and (c) water vapor mixing ratio (g kg^{-1}) in JJA, where "L" represents the land in the reference area, and "O" represents the ocean.

thus the simulated systematic biases are relatively reduced.

4 The impact of air-sea interaction

The impacts of PBL parameterization schemes on the EASM simulation are more sensitive over the ocean, but less over the land. With the further analysis, the simulated upward latent heat flux in the oceanic surface is more in the YSU scheme than that in BouLac (Figure 9(a)), but the incoming solar radiation is less in YSU because of the stronger convective activity (Figure not shown). As a result, the two main terms (latent heat flux and shortwave radiation) of the energy budget at the sea surface will lead to more energy loss from the ocean in YSU scheme. The energy loss certainly reduces the sea surface temperature (SST) in YSU; however, there is no ocean model coupled into WRF and no difference in SST due to the prescribed SST in every PBL scheme run. Consequently, the prescribed SST in YSU scheme plays the role of an increased SST, which can further enhance the release of latent heat, intensify the convective activity and precipitation, and then finally induce the continued growth of the model systemic error. Over the land, however, there is land surface process considered in WRF, so the modeling surface energy budget is more reasonable through the interaction between the land and atmosphere.

Can the consideration of the air-sea interaction in WRF model reduce the biases caused by the PBL schemes? We have coupled an ocean mixed layer model into WRF, and this coupled model can improve the WRF's performance on the simulation of typhoon (Wang et al., 2012). A new ensemble run using the coupled WRF model with YSU PBL scheme is designed (called coupled run). All the model sets in the coupled run are the same with the former uncoupled experiment using YSU scheme; the details of the coupled model can reference Wang et al. (2012). Since the ocean

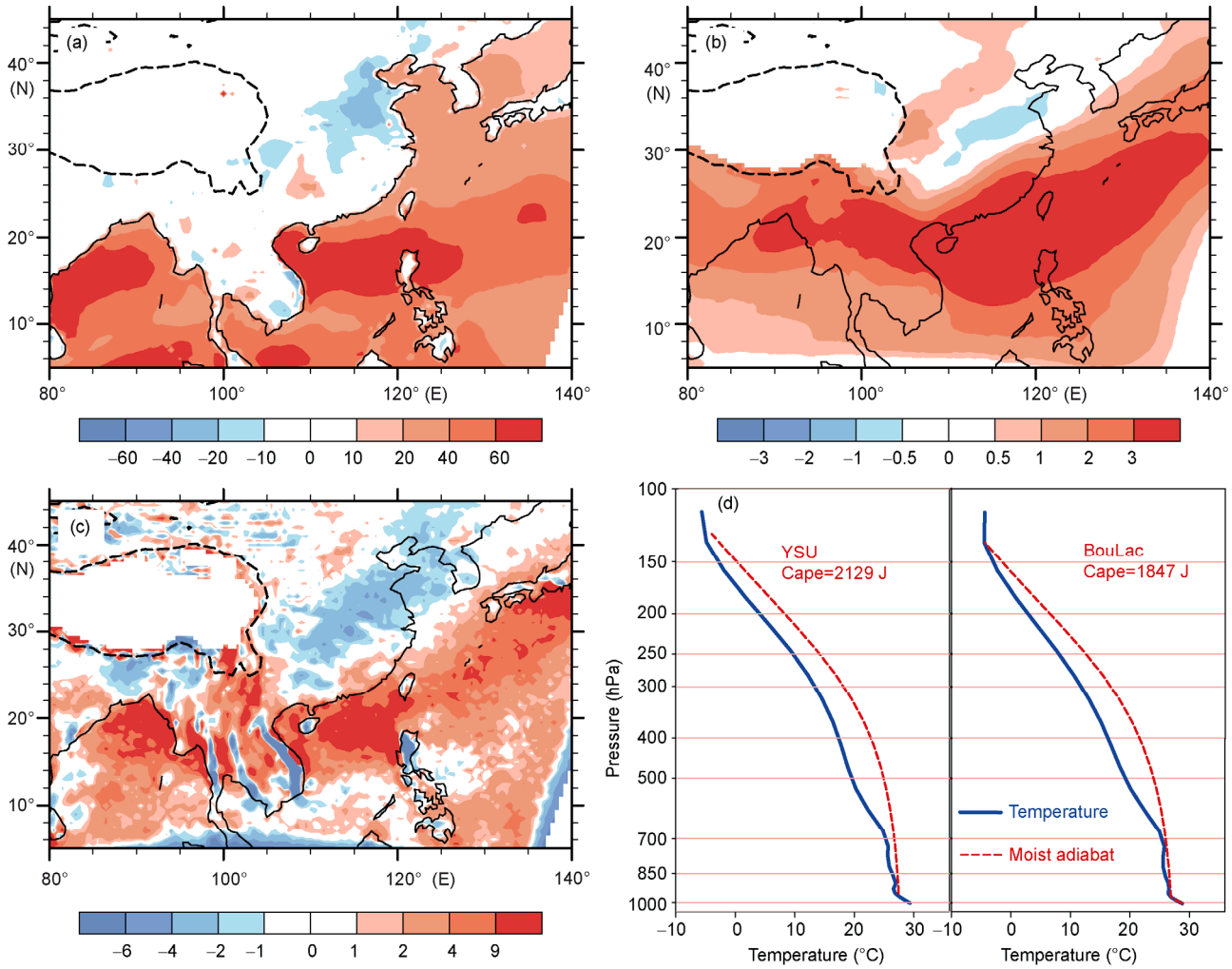

Figure 9 The differences of simulated results between YSU and BouLac in JJA. (a) Latent heat flux (W m^{-2}); (b) E/C_p (°C) at 700 hPa, where E is wet enthalpy, and C_p is the specific heat at constant pressure; (c) the transformed term from CAPE to kinetic energy (10^{-2} J kg^{-1} s^{-1}); (d) the vertical profiles of temperature (blue line) and moist adiabat (red line) (°C) at the reference grid (25°N, 130°E), and the corresponding CAPE (J) in YSU and BouLac, respectively.

model is a one-dimension mixed layer model and the simulation is done during the summer monsoon period, the horizontal transport effect of the ocean cannot be ignored. Thus a nudging method is used to the SST simulation in the coupled run with the observed OISST data (Duan et al., 2008), and the nudging timescale is chosen as 15 days.

Figure 10 shows the differences of the SST, surface latent heat flux and precipitation, and wind at 850 hPa between the coupled and uncoupled runs with YSU scheme. After including the air-sea interaction, the SST simulated with YSU presents a cooling sea surface over the strong convective areas (such as BOB, SCS, and WP, shown in Figure 7). The decreased SST can suppress the development of convection, and weaken the upward release of the latent heat flux (Figure 10(b)). As described in the difference of wind at 850 hPa (Figure 10(c)), the effect of air-sea interaction improves the WPSH simulation, then the southwesterly jet over WP is weakened, and the low-level southwestern monsoon circulation over East China is enhanced significantly. Simultaneously, as to the positive precipitation in Figure 7(b), the YSU scheme reduced the convective precipitation successfully after consideration of the oceanic effect, and the modeling rainfall over the north of Yangtze River is also improved due to the enhancement of simulated southwesterly. The statistic results from the coupled run indicate that the spatial correlation coefficient of precipitation is 0.620 (where it is 0.594 in Table 1), and the RMSE is reduced to be 4.459 mm day^{-1} (where it is 5.320 mm day^{-1} in Table 1).

As previously explained, the performance of EASM simulation with YSU scheme is indeed improved if the ocean model is coupled into WRF, and the biases in both circulation and precipitation caused by the stronger PBL mixing are reduced. Incidentally, because of the importance of the air-sea interaction on the weather or climate simulation (e.g., Wu et al., 2005; Yao et al., 2008; Duan et al., 2008; 2009;

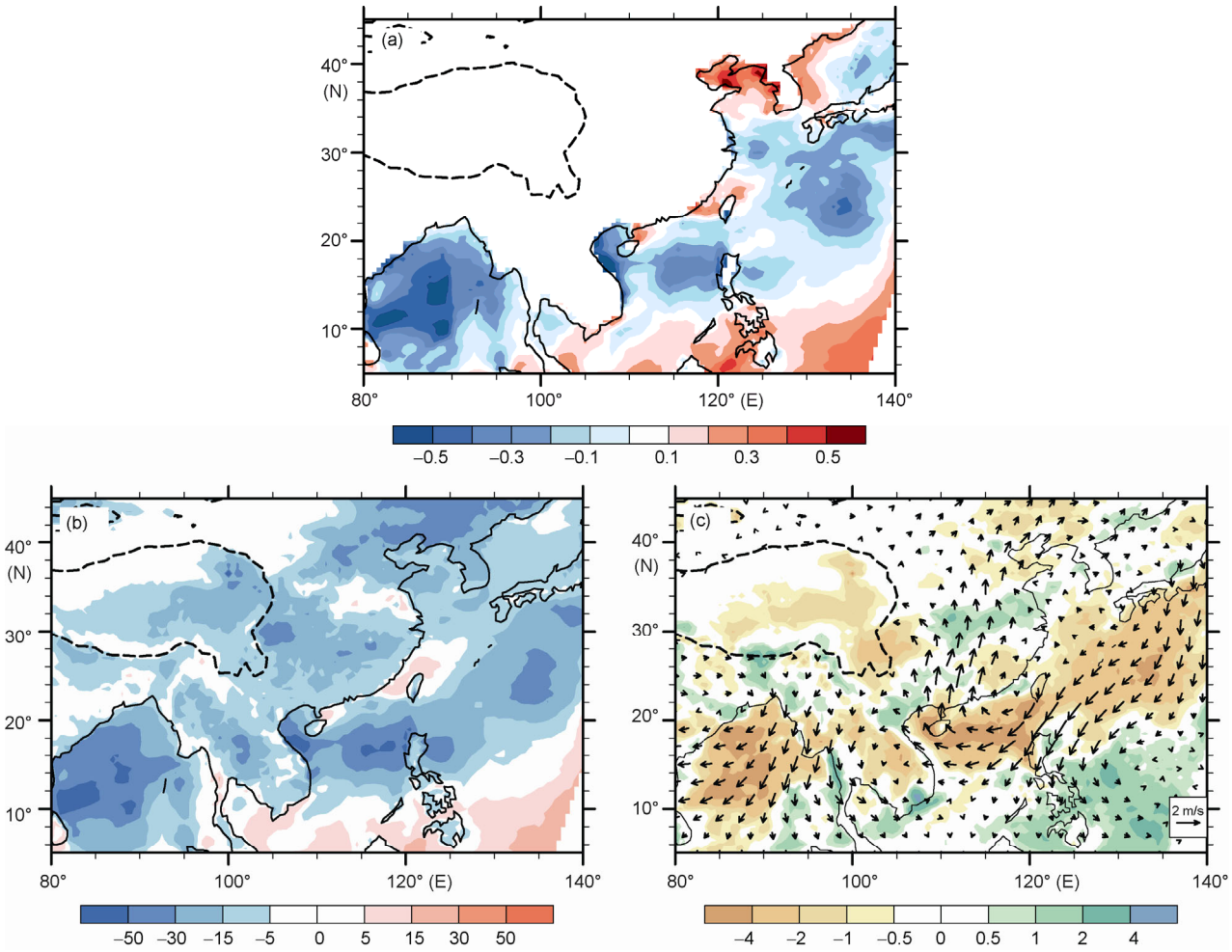

Figure 10 The differences of simulated results between coupled and uncoupled experiments with YSU scheme in JJA. (a) SST (°C); (b) latent heat flux (W m^{-2}); (c) precipitation (shaded, mm day^{-1}) and wind at 850 hPa (m s^{-1}).

Kim et al., 2010; Li et al., 2010; Zou et al., 2011; Peng et al., 2012), no matter which PBL scheme is used in WRF model, the air-sea coupling always has a positive role in the EASM simulation with WRF model.

5 Discussion and summary

Here we investigated the impacts of four widely used PBL schemes (YSU, ACM2, Boulac, and MYJ) and air-sea interaction on the EASM simulation with WRF model. We found that the modeling circulation and precipitation in the nonlocal closure scheme YSU are similar to another nonlocal scheme ACM2; and the results in the other two local TKE schemes (BouLac and MYJ) are also close to each other.

The simulated results of the Boulac and MYJ schemes are more consistent with the observations than those in the YSU and ACM2 schemes. The former reproduce more reasonable low-level southwesterly flow over East China and WPSH than the latter. As to the summer monsoon precipitation, both the spatial distributions and temporal evolutions from Boulac and MYJ are also better than those in YSU and ACM2 schemes. There are dry biases of the simulated precipitation over the Yangtze and Huaihe River basins, and obviously overestimation of precipitation over the ocean and southern coastal area in YSU and ACM2 schemes.

In addition, through the comparison between the YSU and Boulac experiments, the differences from the results of EASM simulation are more obvious over the oceanic area. In the experiments with nonlocal schemes YSU and ACM2, the PBL mixing processes are much stronger, which produce more sea surface upward latent heat flux and stronger convective activity, and finally induce the overestimated precipitation and the corresponding deviation of monsoon circulation. On the contrary, PBL mixing processes in MYJ and BouLac schemes are weaker, and thus the simulated systematic biases are relatively reduced.

We further found that the absence of air-sea interaction in WRF may amplify the biases caused by the PBL scheme over the oceanic region. Through the comparison between the coupled and uncoupled runs with YSU scheme, the pro-

cess of cloud-radiation feedback in the air-sea coupled model can cool the sea surface. The reduced SST weakens the upward latent heat flux and convective activity that are caused by the stronger PBL mixing, and then improves the simulation of monsoon circulation and precipitation.

Furthermore, it should be noted that the results in this study probably are impacted by the other physical parameterization schemes, the model resolution, and the domain size or location. Additionally, the other physical parameterization schemes in WRF such as the impact of cloud-radiation feedback on the EASM simulation are required to be discussed in the future work.

We thank the anonymous reviewers for their constructive comments. This work was jointly sponsored by the "Strategic Priority Research Program—Climate Change: Carbon Budget and Related Issue" of the Chinese Academy of Sciences (Grant No. XDA-05110303), the Opening Fund of Key Laboratory for Land Surface Process and Climate Change in Cold and Arid Regions, CAS, the National Basic Research Program of China (Grant No. 2010CB951703), and the Social Common Weal Profession Research Program of Chinese Ministry of Finance/Ministry of Science and Technology (Grant No. GYHY201006014).

Bougeault P, Lacarrere P. 1989. Parameterization of orographyinduced turbulence in a mesobeta-scale model. Mon Weather Rev, 117: 1872–1890

Cha D-H, Lee D-K, Hong S-Y. 2008. Impact of boundary layer processes on seasonal simulation of the East Asian summer monsoon using a Regional Climate Model. Meteorol Atmos Phys, 100: 53–72

Duan A M, Sui C, Wu G X. 2008. Simulation of local air-sea interaction in the great warm pool and its influence on Asian monsoon. J Geophys Res, 113: D22105

Duan A M, Sui C, Wu G X. 2009. Local air-sea interaction in intertropical convergence zone simulations. J Geophys Res, 114: D22101

Emori S, Nozawa T, Numaguti A, et al. 2001. Importance of cumulus parameterization for precipitation simulation over East Asia in June. J Meteorol Soc Jpn, 79: 939–947

Feng J M, Fu C B. 2007. Inter-comparison of long-term simulations of temperature and precipitation over China by different regional climate models (in Chinese). Chin J Atmos Sci, 31: 805–814

Flaounas E, Bastin S, Janicot S. 2011. Regional climate modeling of the 2006 West African monsoon: Sensitively to convection and planetary boundary layer parameterization using WRF. Clim Dyn, 36: 1083–1105, doi: 10.1007/s00382-010-0785-3

Fu C B, Wang S Y, Xiong Z, et al. 2005. Regional climate model intercomparision project for Asia. Bull Amer Meteorol Soc, 86: 257–266

Giorgi F, Mearns L O. 1999. Introduction to special section: Regional climate modeling revisited. J Geophys Res, 104: 6335–6352

Gochis D J, Shuttleworth, Yang Z L. 2002. Sensitivity of the modeled North American monsoon regional climate to convective parameterization. Mon Weather Rev, 130: 1282–1298

Guan Y. 2010. The influence of air-sea interaction on the formation of monsoon onset vortex over BOB and the Asian monsoon onset (in Chinese). Doctoral Dissertation. Beijing: Graduate University of Chinese Academy of Sciences. 33–37

Holtslag A A M, Boville B A. 1993. Local versus nonlocal boundary-layer diffusion in a global climate model. J Clim, 6: 1825–1825

Hong S Y, Noh Y, Dudhia J. 2006. A new vertical diffusion package with an explicit treatment of entrainment processes. Mon Weather Rev, 134: 2318–2341

Hong S Y, Pan H L. 1996. Non-local boundary layer vertical diffusion in medium-range forecast model. Mon Weather Rev, 124: 1215–1238

Hu X M, Nielsen-Gammon J W, Zhang F. 2010. Evaluation of three planetary boundary layer schemes in the WRF model. J Appl Meteorol Clim, 49: 1831–1844

Huffman G J, Adler R H, Bolvin D T, et al. 2007. The TRMM multi-satellite precipitation analysis: Quasi-global, multi-year, combined-sensor precipitation estimates at fine scale. J Hydrometeorol, 8: 38–55

Janjic, Z I. 1990. The step-mountain coordinate: Physical package. Mon Weather Rev, 118: 1429–1443

Janjic, Z I. 2002. Nonsingular Implementation of the Mellor-Yamada Level 2.5 Scheme in the NCEP Meso model. NCEP Office Note, 437: 61

Kim E J, Hong S Y. 2010. Impact of air-sea interaction on East Asian summer monsoon climate in WRF. J Geophys Res, 115: D19118

Kim H-J, Wang B. 2011. Sensitivity of the WRF model simulation of the East Asian summer monsoon in 1993 to shortwave radiation scheme and ozone absorption. Asia-Pacific J Atmos Sci, 47: 167–180

Lee D-K, Cha D-H, Choi S-J. 2005. A sensitive study of regional climate simulation to convective parameterization scheme for 1998 East Asian summer monsoon. J Terr Atmos Ocean Sci, 16: 989–1015

Li T, Zhou G Q. 2010. Preliminary results of a regional air-sea coupled model over East Asia. Chin Sci Bull, 55: 808–819, doi: 10.1007/s11434- 010-0071-0

Li W J, Ding Y H. 2003. Review and prospect of the East Asian monsoon (in Chinese). Annual Symposium of Chinese Meteorological Society

Liang X Z, Xu M, Yuan X, et al. 2012. Climate-weather research and foresting model (CWRF). Bull Amer Meteorol Soc, 93: 1363–1387

Liu H B. 2012. Numerical simulation of the heavy rainfall in the Yangtze-Huai River Basin during summer 2003 using the WRF model. Atmos Oceanic Sci Lett, 5: 20–25

Liu S Y. 2006. CWRF application in East China monsoon area (in Chinese). Doctoral Dissertation. Nanjing: Nanjing University of Information Science and Technology. 123–124

Liu Y M, Ding Y H. 2001a. Modified mass flux cumulus parameterization scheme and its simulation experiment. Part I: Mass flux scheme and its simulation of the flooding in 1991 (in Chinese). Acta Meteorol Sin, 59: 10–22

Liu Y M, Ding Y H. 2001b. Modified mass flux cumulus parameterization scheme and its simulation experiment. Part II: Cumulus convection of the schemes and the sensitivity experiments of MFS (in Chinese). Acta Meteorol Sin, 59: 129–142

Mao J Y, Wu G X. 2012. Diurnal variations of summer precipitation over the Asian monsoon region as revealed by TRMM satellite data. Sci China Earth Sci, 55: 554-556, doi: 10.1007/s11430-011-4315-x

Margaret L, MuKul T, Dudhia J, et al. 2011. Objective determination of PBL depth for evaluation of PBL schemes. WRF Workshop

Mellor G L, Yamada T. 1982. Development of a turbulence closure model for geophysical fluid problems. Rev Geophys Space Phys, 20: 851–875

Mukhopadhyay P, Taraphdar S, Goswamet B N, et al. 2010. Indian summer monsoon precipitation climatology in a high-resolution regional climate model: Impacts of convective parameterization on systematic biases. Weather Forecast, 25: 369–387

Nielsen-Gammon, J W, Powell C L, Mahoney M J, et al. 2008. Multisensor estimation of mixing heights over a coastal city. J Appl Meteorol Clim, 47: 27–43

Peng S Q, Liu D L, Sun Z B, et al. 2012. Recent advance in regional air-sea coupled models. Sci China Earth Sci, 55: 1391–1405, doi: 10.1007/s11430-012-4386-3

Pleim, J E. 2007a. A combined local and nonlocal closure model for the atmospheric boundary layer, Part I: Model description and testing. J Appl Meteorol Clim, 46: 1383–1395

Pleim, J E. 2007b. A combined local and nonlocal closure model for the atmospheric boundary layer, Part II: Application and evaluation in a mesoscale meteorological model. J Appl Meteorol Clim, 46: 1396–1409

Qort A H. 1964. On estimates of the atmospheric energy cycle. Mon Weather Rev, 92: 483–499

Tao S Y, Li J S, Wang A S. 1997. East Asian monsoon and the flood disaster in China (in Chinese). Disaster Reduction in China, 7: 17–24

Wang B, Yang H W. 2008. Hydrological issues in lateral boundary conditional for regional climate modeling: simulation of East Asian summer

monsoon in 1998. Clim Dyn, 31: 477–490
Wang W, Seaman N L. 1997. A comparison study of convective parameterization schemes in a mesoscale model. Mon Weather Rev, 25: 252–278
Wang Z Q, Duan A M. 2012. A new mixed-layer model coupled into WRF. Atmos Oceanic Sci Lett, 5: 170–175
Wu G X, Guan Y, Liu Y M, et al. 2012. Air-sea interaction and formation of the Asian summer monsoon onset vortex over the Bay of Bengal. Clim Dyn, 38: 261–279
Wu G X, Liu Y M, He B, et al. 2012. Thermal controls on the Asian summer monsoon. Sci Rep, 2: 404
Wu R, Kirtman B P. 2005. Roles of Indian and Pacific Ocean air-sea coupling in tropical atmospheric variability. Clim Dyn, 25: 155–170
Yang H W, Wang B, Wang B. 2011. Reduction of systematic biases in regional climate downscaling through ensemble forcing. Clim Dyn, 38: 655–665, doi: 10.1007/s00382-011-1006-4
Yao S X, Zhang Y C. 2008. Simulation of China summer precipitation with a regional air-sea coupled model (in Chinese). Acta Meteorol Sin, 66: 131–142
Yu E T, Wang H J, Gao Y Q, et al. 2011. Impacts of cumulus convective parameterization schemes on summer monsoon precipitation simulation over China. Acta Meteorol Sin, 25: 581–592
Zhang D L, Zheng W Z. 2004. Diurnal cycles of surface winds and temperatures as simulated by five boundary layer parameterizations. J Appl Meteorol, 43: 157–169
Zhu Q G, Lin J R, Shou S W, et al. 2000. Synoptic Theory and Method (version 3) (in Chinese). Beijing: China Meteorological Press. 474
Zou L W, Zhou T J. 2012. Development and evaluation of a regional ocean-atmosphere coupled model with focus on the western North Pacific summer monsoon simulation: Impacts of different atmospheric components. Sci China Earth Sci, 55: 802–815, doi: 10.1007/s11430-011-4281-3